M.Sabuncu [1], H.Ozturk [2], S.Cimen [3]

OUT-OF-PLANE DYNAMIC STABILITY ANALYSIS OF CURVED BEAMS SUBJECTED TO UNIFORMLY DISTRIBUTED RADIAL LOADING

Dokuz Eylul University, Faculty of Engineering, Department of Mechanical Engineering, 35100 Bornova, Izmır, Turkey; e-mail: [1] *mustafa.sabuncu@deu.edu.tr;* [2] *hasan.ozturk@deu.edu.tr;* [3] *serefcimen@gmail.com*

Abstract The out-of-plane stability of tapered cross-sectioned thin curved beams under uniformly distributed radial loading is investigated by using the Finite Element Method. Solutions referred to as Bolotin's approach are investigated for the dynamic stability analysis and the first unstable regions are examined. Out-of-plane vibrations and out-plane buckling analyses are also considered. In addition, the results obtained in this study are compared with the results of other investigators in existing literature for the fundamental frequency and critical lateral buckling load. The effects of subtended angle, variations of cross-section and dynamic load parameter on the stability regions are shown in graphics

Key words: dynamic stability, finite elements, buckling, curved beam, vibration.

§1. Introduction.

Curved beams are used in high technology applications especially in turbine blades, bridges and outer space industry and this has made elastic instability a problem of great importance. The problems, which are examined in this branch of elasticity, are related to those in the theory of vibrations and the stability of elastic systems. The dynamic stability of mechanical systems according to Bolotin's definition [4], represents a specific stability of motion. When Bolotin's approach [4] examined, three stages, static stability (buckling analysis), vibration analysis and dynamic stability analysis, are seen to be included in the equation of dynamic stability. Therefore, these three stages are studied in this paper. Some of the research studies on the dynamic and static stabilities of structures that have been carried out by other investigators can be summarized as follows:

Timoshenko and Gere [21] studied the buckling analysis of hinged-hinged Bernoulli-Euler curved beams by using the analytical method. Papangelis & Trahair [15] developed a flexural-torsional buckling theory for circular arches of doubly symmetric cross section. Non linear expressions for the axial and shear strains were derived, and these were substituted into the second variation of the total potential to obtain the buckling equation. Banan et al [1] discussed the Finite Element analysis for the buckling analysis of curved beams on elastic foundations for both in-plane and out-plane. Bazant and Cedolin [2] examined the buckling analysis of curved beams by employing analytical and energy methods. Yoo et al [27] performed buckling analysis of curved beams by using the finite element method. Tüfekci and Arpacı [22] studied exact analytical solutions for in-plane static problems of planar curved beams with variable curvatures and variable cross-sections which are derived by using the initial value method. The governing equations include the axial extension and shear deformation effects.

Ojalvo & Newman [13], presented the frequencies of a cantilever ring segment. Sabir and Ashwel [17] discussed the natural frequency analysis of circular aches deformed in plane. The finite elements developed by using different types of shape functions are employed in their analysis. Petyt and Fleischer [16] analyzed free vibrations of a curved beam

for various boundary conditions. Belek [3] studied the vibration characteristics of a symmetrical cross section curved packet. The effect of disc curvature on the frequencies of vibration was investigated and was shown that the vibration characteristics of a multi-bladed packet can be predicted from the in-plane and out-of-plane inference diagrams of a symmetric cross section two bladed curved packet. Sabuncu [18] investigated the vibration analysis of thin curved beams. He used several types of shape functions to develop different curved beam finite elements and pointed out the effect of displacement functions on the natural frequencies by comparing the results. Silva and Urgueira [19] studied the dynamic stiffness matrices for the out-of-plane vibration of curved beams using the Lagrange's equations and the dynamic equilibrium equations, respectively, and then solved for the natural frequencies. Kang et al [7] discussed computation of the eigenvalues of the equations of motion governing the free in plane vibration including extensibility of the arch axis and the coupled out-of-plane twist-bending vibrations of circular arches using Differential Quadrature methods (DQM). Kawakami et al [8] derived the characteristic equation by applying the discrete Green functions and using the numerical integration to obtain the eigenvalues for both the in-plane and out-of-plane free vibrations of the non-uniform curved beams, where the formulation is much complicated than that of the classical approaches. Yıldırım [26] performed the in-plane and out-plane free vibration analysis with the program developed using the transfer matrix method of a double-side symmetric and elastic curved beam. Huang et al [6] investigated a systematic method for analyzing the out-of-plane dynamic behaviours of non-circular curved beams the governing equations of which take into account the effects of shear deformation, rotary inertia and viscous damping. Wang and Sang [23] derived an analytic method of examining the out-of-plane vibration of continuous curved beams on periodical supports. Lee and Chao [10, 11] examined out-plane vibration of curved beams with a non-uniform cross-section for constant angle and two physical parameters are introduced to simplify the analysis, and the explicit relations between the torsional displacement, its derivative and the flexural displacement were derived. Wu and Chiang [24] investigated the natural frequencies and mode shapes for the radial bending vibrations of uniform circular arches by means of curved beam elements. In this study, the standard techniques were used to determine the natural frequencies and mode shapes for the curved beam with various boundary conditions and subtended angles. An improved shear deformable thin-walled curved beam theory to overcome the drawback of currently available beam theories was newly proposed for the spatially coupled free vibration and elastic analysis by Kim and Kim [9]. The governing differential equations for the free in-plane vibration of uniform and non-uniform curved beams with variable curvatures, including the effects of the axis extensibility, shear deformation and the rotary inertia, were derived using the extended-Hamilton principle by Yang et al [25].

Thomas and Abbas [20] examined dynamic stability of an axial periodic loaded Timoshenko beam using the finite element method and Bolotin's approach [4]. In this study the effect of shear deformation and rotary inertia on the static buckling loads and the regions of dynamic instability were studied. Nair et al [12] investigated the dynamic stability of a curved rail under a constant moving load using a linear theory. Fukuchi and Tanaka [5] studied a characteristic analysis on quasi-periodic and chaotic behavior of a circular arch under follower forces with small disturbances. In this study, the stability region chart of the disturbed equilibrium in an excitation field was calculated numerically. Ozturk, et al [14] have investigated in-plane stability analysis of non-uniform cross-sectioned thin curved beams under uniformly distributed dynamic loads by using the Finite Element Method. In this study, two different finite element models, representing variations of cross-section, were developed by using simple strain functions in the analysis.

This paper presents the out-of-plane stability analysis of tapered cross-sectioned thin curved beams under uniformly distributed radial loading by using the Finite Element Method. Solutions referred to as Bolotin's approach are investigated for the dynamic stability analysis and the first unstable regions are examined. Since natural frequency and buckling load effect the determination of stability regions, the out-of-plane vibration and lateral buckling analyses are also studied. In addition the results obtained from this study are compared with the results of other investigators in existing literature for the fundamental frequency and critical lateral buckling load. The effects of subtended angle, variations of cross-section and dynamic load parameter on the stability regions are shown in graphics.

§2. Models of Curved Beams.

The model shown in Fig. 1is used for the Finite Element analysis of curved beams. In this study, C1, C2, C3, C4 and C5, represent different type cross-sectioned curved beams. The explanation of these cross-sections is as follows:

C1: Uniform ($t_R = t_t$, $b_R = b_t$; Fig. 2a);

C2: Unsymmetric tapered with constant width ($t_R \neq t_t$, $b_R = b_t$; Fig. 2b.),

C3: Double unsymmetric tapered ($t_R \neq t_t$, $b_R \neq b_t$; Fig. 2c.),

C4: Symmetric tapered with constant width ($t_R \neq t_t$, $b_R = b_t$; Fig. 2d.),

C5: Double symmetric tapered ($t_R \neq t_t$, $b_R \neq b_t$ Fig 2e.).

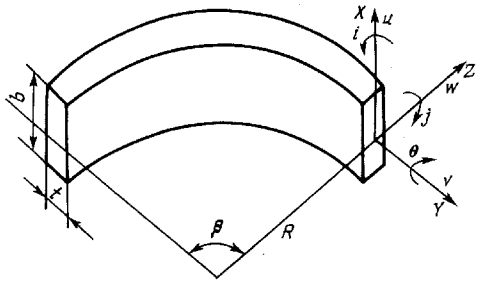

Fig. 1 Coordinate system and displacements of the curved beam.

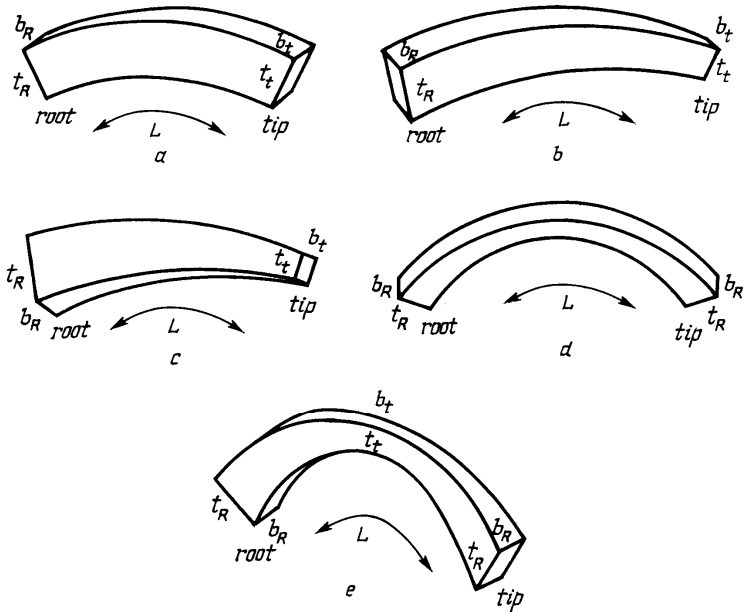

Fig. 2. Cross-sections of curved beams (a) uniform (C1, $t_R = t_t$, $b_R = b_t$); unsymmetric tapered with constant width (C2, $t_R \neq t_t$, $b_R = b_t$); (c) double unsymmetric tapered (C3, $t_R \neq t_t$, $b_R \neq b_t$.); (d) symmetric tapered with constant width(C4, $t_R \neq t_t$, $b_R = b_t$); (e) double symmetric tapered (C5, $t_R \neq t_t$, $b_R \neq b_t$).

The boundary conditions and applied loading on a curved beam are shown in Fig. 3. The periodic uniformly distributed dynamic load is $P(t) = P_0 + \ +P_t \cos wt$ where ω is the disturbing frequency, the static and time dependent components of the load can be represented as a fraction of the fundamental static buckling load P_{cr}, hence $P(t)$ becomes,

$$P(t) = P_{cr}(a + b_d \cos wt). \qquad (2.1)$$

The displacement functions of the curved beam were defined as [3];

$$u = a_1 R\cos f + a_2 R\sin f + a_3 R - a_4 Rf - a_6 Rf\,; \quad (2.2)$$

$$q = a_1 \cos f + a_2 \sin f - a_5 - a_6 f\,; \qquad (2.3)$$

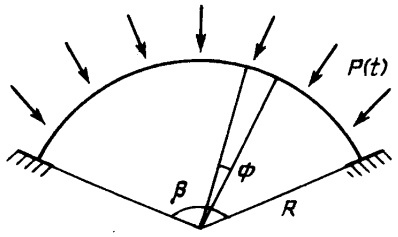

Fig. 3. Curved beam under uniformly distributed radial loading.

$$f = y/R. \tag{2.4}$$

Generalize coordinate vector of an element is obtained by Using Eqs. (2) and (3) for FEM

$$\{q_o\}^T = [q_i \;\; u_i \;\; j_i \;\;\; q_{i+1} \;\;\; u_{i+1} \;\; j_{i+1}], \tag{2.5}$$

where q_i u_i and j_i are torsional displacement, displacement in X direction and slope of u deflection in the i^{th} node, respectively

$$j = -\frac{\partial u}{\partial y}. \tag{2.6}$$

If the terms in Eq. (A.13) in the Appendix are substituted in the energy equations below, for a finite element, Elastic Stiffness Matrix, Geometric Stiffness Matrix and Mass Matrix are obtained, respectively.

The strain energy of the curved beam element is [3],

$$V_o = \frac{1}{2}\int_0^{l_{sh}} \left[EI_z \left(u'' + \frac{q}{R} \right)^2 + GJ \left(q' - \frac{u'}{R} \right)^2 \right] dy, \tag{2.7}$$

where $q' = \frac{\partial q}{\partial y}$, $u' = \frac{\partial u}{\partial y}$ and $u'' = \frac{\partial^2 u}{\partial y^2}$,

$$V_o = \frac{1}{2}\{q_o\}^T [C_o]^{-T} [kk_o][C_o]^{-1}\{q_o\} \rightarrow k_o = [C_o]^{-T} [kk_o][C_o]^{-1}, \tag{2.8}$$

where k_0 is the elastic stiffness matrix of a single element ($[kk_o]$ given in Appendix).

The kinetic energy of the curved beam element is [3],

$$T_o = \frac{1}{2}\int_0^{l_{sh}} \left[r\,A(\dot{u})^2 + r\,I_p(\dot{q})^2 \right] dy; \tag{2.9}$$

$$T_o = \frac{1}{2}\{\dot{q}_o\}^T [C_o]^{-T} [mm_o][C_o]^{-1}\{\dot{q}_o\} \;\; m_o = [C_o]^{-T} [mm_o][C_o]^{-1}, \tag{2.10}$$

where m_0 is the mass matrix of a single element ($[mm_o]$ given in Appendix). V_{go} denotes the external work done by a uniformly distributed radial loading $P(t)$ and given by the equation [15],

$$V_{go} = \frac{1}{2}\int_0^{l_{sh}} P(t)R \left[u'^2 + r_x^2 q'^2 + r_z^2 \left(q' - \frac{u'}{R} \right)^2 \right] dy; \tag{2.11}$$

$$r_x^2 = \frac{I_x}{A}; \;\; r_z^2 = \frac{I_z}{A}, \tag{2.12}$$

where r_x and r_z are the in-plane and out plane radii of gyration.

Eqs. (2.2) and (2.3) are substituted in to Eq. (2.11) and replacing the coefficients $a_1 \ldots a_6$ the

$$V_{go} = \frac{1}{2}\{q_o\}^T P(t)[C_o]^{-T} \left[kk_{go} \right] [C_o]^{-1}\{q_o\} \rightarrow \;\; k_{go} = [C_o]^{-T} \left[kk_{go} \right][C_o]^{-1}, \tag{2.13}$$

where k_{go} is the geometric matrix of a single element ($[kk_{go}]$ given in Appendix).

Mass, elastic stiffness, geometric matrices of each beam element are used to form global mass, elastic stiffness and geometric matrices. The dynamic response of a beam for a conservative system can be formulated by means of Lagrange's equation of motion in which the external forces expressed in terms of time-depended potentials, and then performing the required operations the entire system leads to the governing equation of motion.

$$[M]\{\ddot{q}\}+\left[[K_e]-P(t)\left[K_g\right]\right]\{q\}=0, \tag{2.14}$$

when $P(t)$ is substituted in equation Eq. (2.14). It becomes [20],

$$[M]\{\ddot{q}\}+\left[[K_e]-a\,P_{cr}\left[K_{gs}\right]-b_d P_{cr}\cos wt\left[K_g\right]\right]\{q\}=0. \tag{2.15}$$

Where, K_{gs} and K_{gt} matrices have shown influence of static and time dependent components of the load respectively. Eq. (2.15) represents a system of second order differential equation with periodic coefficients of the Mathieu – Hill type. From the theory of linear equations with periodic coefficients, the boundaries between stable and unstable solutions of Eq. (2.15) are formed by periodic solutions of period T and 2T where $T=2p/w$. It was shown by Bolotin [4] that solutions with period 2T are the ones of greatest practical importance and that as a first approximation the boundaries of the principal regions of the dynamic instability can be determined from the equation:

$$\left[K_e-a\,P_{cr}K_{gs}\pm\frac{1}{2}b_d P_{cr}K_{gt}-\frac{w^2}{4}M\right]q=0. \tag{2.16}$$

The two matrices K_{gs} and K_{gt} will be identical if the static and time dependent component of the loads are applied in the same manner $\left[K_{gs}\right]\equiv\left[K_{gt}\right]\equiv\left[K_g\right]$ then Eq. (2.16) becomes

$$\left[[K_e]-\left(a\pm\frac{1}{2}b_d\right)P_{cr}\left[K_g\right]-\frac{w^2}{4}[M]\right]\{q\}=0: \tag{2.17}$$

(i) Free vibration with $a=0, b_d=0$ and $p=w/2$ the natural frequency

$$\left[[K_e]-p^2[M]\right]\{q\}=0; \tag{2.18}$$

(ii) Static stability with $a=1, b_d=0$ and $w=0$

$$\left[[K_e]-P_{cr}\left[K_g\right]\right]\{q\}=0; \tag{2.19}$$

(iii) Dynamic stability when all terms are present

$$\left[[K_e]-\left(a\pm\frac{1}{2}b_d\right)P_{cr}\left[K_g\right]-\frac{w^2}{4}[M]\right]\{q\}=0. \tag{2.20}$$

§3. Results and discussion.

The first four natural frequencies obtained with the present element are compared with the analytical results of Ojalvo and Newman [13] and given in Table 1. Throughout this investigation, 12 elements are used in modelling the beams. In addition, the critical lateral buckling load of a uniform cross-section beam for various subtended angles are compared with the results of Timoshenko and Gere [21] and given in Table 2.

As seen from Table 1 and Table 2, the agreement between the results obtained by using the present finite element model and exact solution is good.

Table 1

Mode	Natural Frequency (Hz)	
	Present	Ref. [13]
1	9,7	8,48
2	23,19	22,26
3	70,48	72,56
4	176,46	171,5

Table 2

Subtended Angle	Critical Lateral Buckling Load(P_{cr})(kN/m)	
	Present	Ref. [21]
30°	1815,79	1814,8
45°	777,73	775,40
60°	418,70	413,01
90°	167,71	164,1

Table 1. Comparison of the first four natural frequencies of a cantilever curved beam obtained by using the present finite element method and the results of Ojalvo and Newman [13]. (t = 0.0127 m, b = 0.0127 m, R = 0.0254 m, r = 2770 kg/m^3, E = 6.89e10 N/m^2, q = 270°).

Table 2. Comparison of the critical lateral buckling load obtained for various subtended angles of a fixed-fixed curved beam with the results of Timoshenko and Gere [21] (t = 0.001587 m, b = 0.02753 m, R =0.3556 m).

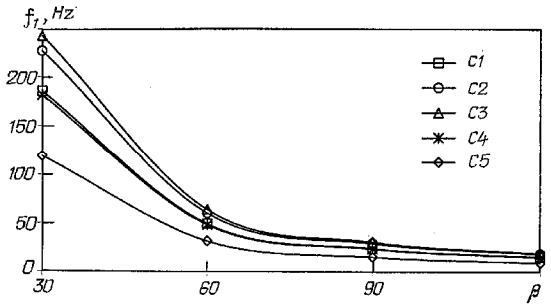

Fig. 4. The effect of variation of subtended angle of an arch on the fundamental frequency for various cross-sections. b_R/b_t = $=t_R/t_t$=1(□ C1), b_R/b_t = 1and t_R/t_t = 0.5(O C2 and * C4), b_R/b_t = = t_R/t_t =0.5(Δ C3 and ◊ C5).

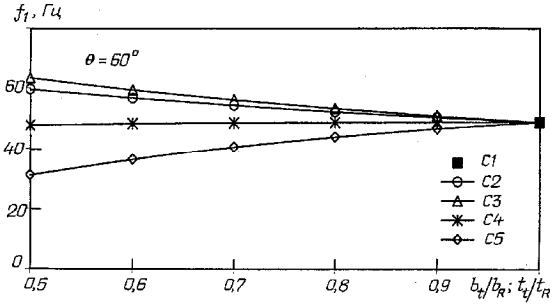

Fig. 5. The variation of the free vibration frequency with various ratio of cross-section. $\theta = 60^\circ$, $b_R=b_t$, $t_R=t_t$ (■ C1), $b_R = b_t$ and $t_R \neq t_t$ (O C2 and * C4), $b_R/b_t = t_R/t_t = 0.5$ (Δ C3 and ◊ C5).

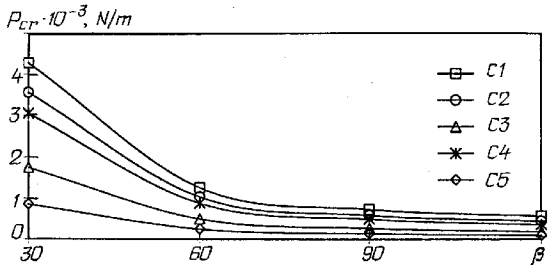

Fig. 6. The variation of the critical lateral buckling load with various cross-section and curve radius. $b_R/b_t = t_R/t_t$=1(□ C1), b_R/b_t = 1 and t_R/t_t = 0.5(O C2 and * C4), $b_R/b_t = t_R/t_t$ = 0.5 (Δ C3 and ◊C5).

Fig. 4 shows that the effect of variation of subtended angle of an arch on the fundamental frequency for various cross-sections. It can be noticed from the figure that when the subtended angle of an arch increases, the fundamental frequency decreases for all the cross-sections as expected. It can also be noticed that the frequency parameters of C2, C3 and C1, C4 cross-sectioned curved beams are fairly close. Between 30° and 60° subtended angles, the fundamental frequency of C5 cross-sectioned curved beams are more apart than the fundamental frequencies of other type cross-sectioned curved beams.

When the subtended angle of an arch increases, the fundamental frequency of curved beams having the same length but five different cross-sections come closer. This phenomenon can be explained as follows: when the subtended angle of an arch increases, the length of curved beams also increases, consequently beams become very flexible. The length variation effect on the flexibility is more dominant than the effect of variation of cross-section.

As shown in Fig. 5, if the variation of the cross-section diminishes and approaches the uniform cross-section, the fundamental frequencies of C4 and C5 cross-sectioned curved beams increase and approach the frequency parameter of C1 cross-sectioned curved beam. On the other hand, the fundamental frequencies of C2 and C3 cross-sectioned curved

beams decrease and approach the fundamental frequency of the C1 cross-sectioned curved beam.

Effect of subtended angle of curvature on the critical lateral buckling load is shown in Figure 6. When the subtended angle of an arch increases, as a result the curved beam becomes more flexible. Thus, as shown in the figure, the critical lateral buckling load decreases. It can be noticed from the figure that critical lateral buckling load values of beams having C1, C2 and C4 type cross-sections are close to each other. There is a similar phenomenon between C3 and C5 type cross-sectioned curved beams. Critical buckling loads of single tapered curved beams (C2 and C4) are higher than the double tapered curved beams (C3 and C5), respectively, as expected. It can also be noticed that even though the thickness of C4 tapers twice as much as C2 and the thickness and width of C5 tapers twice as much as C3 type beams. It seems that symmetric tapered beams are more stable than expected.

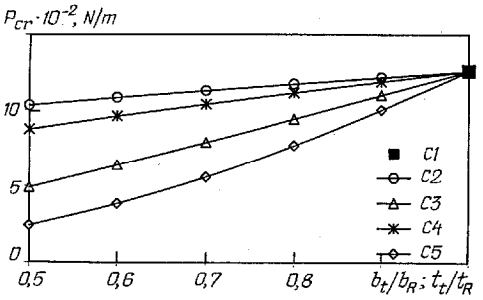

Fig. 7. The variation of the critical lateral buckling load with various ratio of cross-section. $\theta = 60^{\circ}$, $b_R = b_t$, $t_R = t_t$(■ C1), $b_R = b_t$ and $t_R \neq t_t$ (O C2 and * C4), $b_R/b_t = t_R/t_t = 0.5$ (Δ C3 and ◊ C5).

Fig. 7 shows the effect of thickness variation of a curved beam on the critical lateral buckling load for various cross-sections. It is seen that when the variation of cross-section diminishes and approaches the uniform cross-section, the curved beam becomes stiffer; as a result, the critical buckling load increases and takes the value of the uniform cross-sectioned curved beam. From this figure, it can be said that static stability values of curved beams having C5, C3, C4 and C2 type cross-sections increase, respectively. This increase decreases as the cross-section variation diminishes.

From Fig. 8, it can be noticed that the first dynamic instability region widens because of the decrease in the subtended angle of the arch. C3 cross-sectioned curved beam is less stable compared to other cross-sections. In addition, when the dynamic load parameter increases, the unstable region widens.

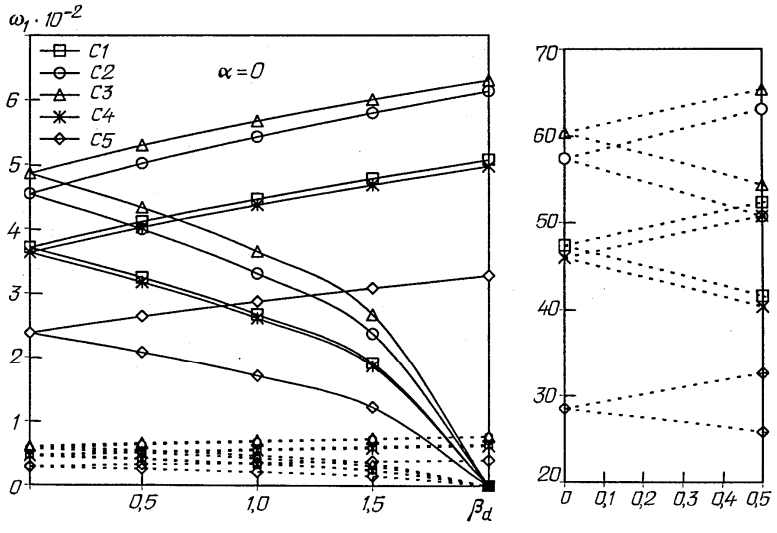

Fig. 8. The effect of dynamic load parameter on the first dynamic stability region of curved beams for various cross-sections and two different subtended angles. $a = 0$ $b_R = b_t$, $t_R = t_t$ (□ C1), $b_R = b_t$ and $t_R \neq t_t$, (O C2 and * C4), $b_R/b_t = t_R/t_t = 0.5$ (Δ C3 and ◊ C5), …… $b = 90^{\circ}$, —— $b = 30^{\circ}$.

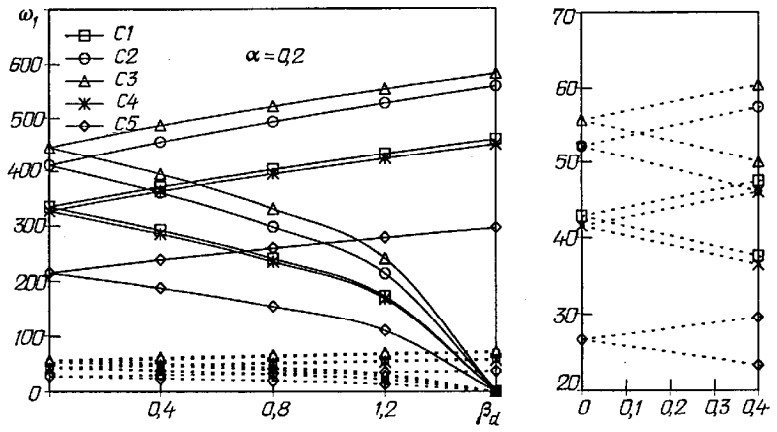

Fig. 9. The effect of dynamic load parameter on the first dynamic stability region of curved beams for various cross-sections and two different subtended angles. $a = 0.2$ $b_R = b_t$, $t_R = t_t$ (□ C1), $b_R = b_t$ and $t_R \neq t_t$, (O C2 and * C4), $b_R/b_t = t_R/t_t = 0.5$ (Δ C3 and ◊ C5), …… $b = 90^\circ$, —— $b = 30^\circ$.

Comparison of Fig. 8 and Fig 9 shows that, if the static load parameter increases, the initial ratio of the disturbing frequency to the fundamental frequency moves towards origin. It can be seen from the figures that the curved beam under periodic loading becomes unstable at a small disturbing frequency and small dynamic load parameter.

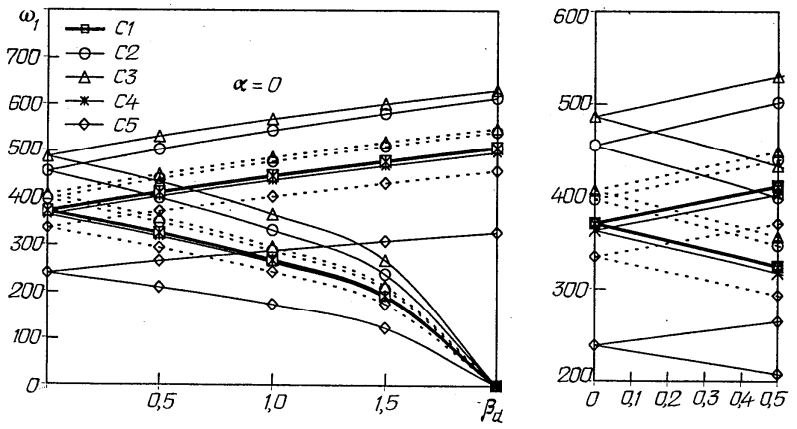

Fig. 10. The effect of dynamic load parameter on the first dynamic stability region of curved beams for various cross-sections and two different subtended angles. $a = 0$, $b = 30^\circ$, —— $b_R/b_t = t_R/t_t = 1$(□ C1), ——— $b_R/b_t = 1$ and $t_R/t_t = 0.5$ (O C2 and * C4), $b_R/b_t = t_R/t_t = = 0.5$ (Δ C3 and ◊ C5), ……. $b_R/b_t = t_R/t_t = 1$(□ C1), $b_R/b_t = 1$ and $t_R/t_t = 0.8$ (O C2 and * C4), $b_R/b_t = t_R/t_t = 0.8$ (Δ C3 and ◊ C5).

Figs. 10 and 11 show that when b_1/b_2 and t_1/t_2 ratios approach unity for $a = 0$ and $a = 0,2$, the first unstable region approaches the region of C1 cross-sectioned curved beam. For both figures, the order of the unstable regions of all cross-sections does not change from the stability point of view.

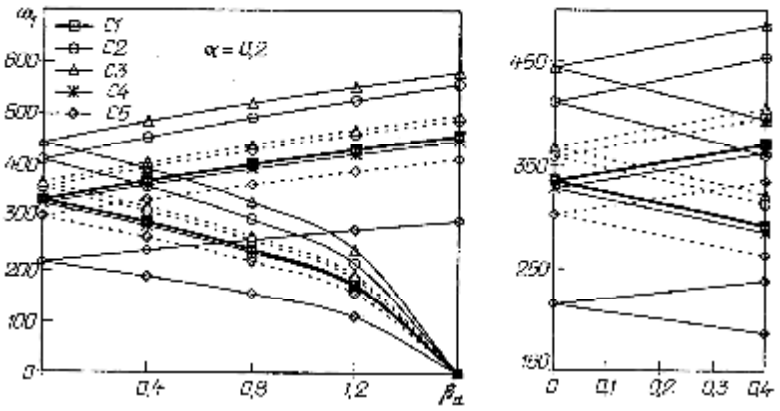

Fig. 11. The effect of dynamic load parameter on the first dynamic stability region of curved beams for various cross-sections and two different subtended angles. a = 0.2, b = 30˚, —— $b_R/b_t = t_R/t_t$ =1(□ C1), ——— b_R/b_t = 1 and t_R/t_t = 0.5 (O C2 and * C4), $b_R/b_t = t_R/t_t$ = 0.5 (Δ C3 and ◊ C5) , ……. $b_R/b_t = t_R/t_t$=1(□ C1), b_R/b_t = 1 and t_R/t_t = 0.8 (O C2 and * C4), $b_R/b_t = t_R/t_t$ = 0.8 (Δ C3 and ◊ C5).

§4. Conclusions.

This paper presents the dynamic and static stability of non-uniform cross-sectioned curved beams. The finite element method has been employed in the analysis. The effects of subtended angle, variations of cross-section and dynamic load parameter on the out-plane stability regions are examined. When the subtended angle of an arch increases the static stability (buckling) decreases and dynamic instability region widens but the initial ratio of the disturbing frequency to the fundamental frequency moves up from the origin. If the static load parameter is equal to 0.2, initial disturbing frequency moves towards origin. However, the dynamic load parameter is bounded between the values of zero and 1.6. Consequently, by changing the static and dynamic load parameters and the ratios of dimensions of thickness and width at the tip cross-section to the ones at the root cross-section, the out-plane dynamic stability of curved beam may be conserved.

Nomenclature:

A : Area of curved beam cross section; b_1 : Width at the root of the curved beam;

b_2 : Width at the top of the curved beam; E : Modulus of elasticity of curved beam;

f : Natural frequency; G : Shear modulus of curved beam;

I_p : Polar moment of area of cross-section; I_x : Second moment of area of cross section about axis X; I_z : Second moment of area of cross section about axis Z;

J : St. Venant torsion constant of a curved beam; l_{sh} : Length of beam element;

R : Radius of curved beam; t_1 : Thickness at the root of the curved beam;

t_2 : Thickness at the top of the curved beam; $[K]$: Global elastic stiffness matrix;

$[K_{go}]$: Global geometric matrix; $[M]$: Global mass (inertia) matrix;

a : Static component of load; b : Subtended angle; b_d : Dynamic component of load;

r : Density of curved beam.

Р Е З Ю М Е . За допомогою методу скінчених елементів проаналізовано бокову стійкість викривленої звуженої у кінці тонкої балки при однорідно розподіленому радіальному навантаженні. Розв‘язки у вигляді наближення Болотіна досліджені в рамках аналізу динамічної стійкості. Також вивчені бокові коливання і бокове випучення балки. Отримані результати щодо основної частоти та критичного навантаження при боковому випученні порівняні з іншими опублікованими результатами. На рисунках показано вплив утвореного дугою кута зміни поперечного перерізу та параметру динамічного навантаження на область стійкості.

1. *Banan, M. R., Karami, G., Farshad, M.* Finite element stability analysis of curved beams on elastic foundation // Math. Comput. Model. – 1990. – **14**. – P. 863 – 867.

2. *Bazant, Z.P., Cedolin, L.* Stability of structures. – New York: Oxford University Press, 1991.

3. *Belek, H.T.* Vibration characteristics of shrouded blades on rigid and flexible disks.– England: University of Surrey, Ph D. Thesis, 1977.

4. *Bolotin, V.V.* Dynamic stability of elastic systems. – San Francisco: Holden Day, 1964.

5. *Fukuchi, N., Tanaka, T.* Non-periodic motions and fractals of a circular arch under follower forces with small disturbances // Steel Compos. Struct.– 2006. – **6**, N 2. – P. 87 – 101.

6. *Huang, C.S., Tseng, Y.P., Chang, S.H.* Out-of-plane dynamic response of non circular curved beams by numerical laplace transform // J. Sound Vib. – 1998. – **215**, N3. – P. 40 – 424.

7. *Kang, K.J., Bert, C.W., Striz, A.G.* Vibration and buckling analysis of circular arches using DQM // Comput. Struct. – 1995. – **60**, N 1. – P. 49 – 57.

8. *Kawakami, M., Sakiyama, T., Matsuda, H., Morita, C.* In-plane and out- of- plane free vibrations of curved beams with variable cross sections // J. Sound Vib. – 1995. – **187**, N 3. – P. 381 – 401.

9. *Kim, N.I., Kim, M.Y.* Free vibration and elastic analysis of shear-deformable non-symmetric thin-walled curved beams: A centroid-shear center formulation // Struct. Eng. Mech. – 2005. – **21**, N 1. – P. 19 – 33.

10. *Lee, S.Y., Chao, J.C.* Out-of-plane vibrations of curved non-uniform beams of constant radius // J. Sound Vib. – 2000. – **238**, N 3. – P. 443 – 458.

11. *Lee, S.Y., Chao, J.C.* Exact solutions for out-of-plane vibration of curved nonuniform beams // J. Appl. Mech.-T ASME. – 2001. – **68**, N 2. – P. 186 – 191.

12. *Nair, S., Garg, V.K., Lai, Y.S.* Dynamic stability of a curved rail under a moving load // Appl. Math. Model. – 1985. – **9**. – P. 220 – 224.

13. *Ojalvo, I.U., Newman, M.* Natural frequencies of clamped ring segments // Machine Design. – 1964. – **21**. – P. 219 – 220.

14. *Ozturk, H., Yesilyurt, I., Sabuncu, M.* In plane analysis of non-uniform cross-sectioned curved beams // J. Sound Vib. – 2006. – **296**, N 1 – 2. – P. 277 – 291.

15. *Papangelis, J.P., Trahair, N.S.* Flexural-torsional buckling of arches // J. Struct Eng. – 1987. – **113**. N 4. – P. 889 – 906.

16. *Petyt, M., Fleischer, C.C.* Free vibration of curved beam // J. Sound Vib. – 1971. – **18**, N 1. – P. 17 – 30.

17. *Sabir, A.B., Ashwell, D.G.* A comparasion of curved beam finite elements when used in vibration problem // J. Sound Vib. – 1971. – **18**. – P. 555 – 563.

18. *Sabuncu, M.* Vibration characteristics of rotating aerofoil cross-section bladed-disc assembly. –England: University of Surrey, Ph D. Thesis, 1978.

19. *Silva, J.M., Urgueira, P.V.* Out of plane dynamic response of curved beams an analytical model // Int. J. Solids Struct. – 1988. – **24**, N 3. – P. 271 – 284.

20. *Thomas, J., Abbas, B.A.H.* Dynamic stability of timoshenko beam by finite element method // J. Eng. Ind. Trans. ASME. **–** 1976. – **98**. – P. 1145 – 1151.

21. *Timoshenko, S. P., Gere, J. M.* Theory of elastic stability. – New York: McGraw- Hill Book Company, 1961.

22. *Tüfekci, E., Arpaci A.* Analytical solutions of in-plane static problems for non-uniform curved beams including axial and shear deformations // Struct. Eng. Mech. – 2006. – **22**, N 2. – P. 131 – 150.

23. *Wang, R.T., Sang, Y.L.* Out-of-plane vibration of multi-span curved beam due to moving loads // Struct. Eng. Mech. – 1999. – **7**, N 4. – P. 361 – 375.

24. *Wu, J. S., Chiang, L.K.* Free vibration analysis of arches using curved beam elements // Int. J. Numer. Meth. Eng. – 2003. – **58**. – P. 1907 – 1936.

25. *Yang, F., Sedaghati, R., Esmailzadeh, E.* Free in-plane vibration of general curved beams using finite element method // J. Sound Vib. – 2008. – **318**, N 4 – 5. – P. 850 – 867.

26. *Yıldırım, V.* A computer program for the free vibration analysis of elastic arcs // Comput. Struct. –1996. – **62**, N 3. – P. 475 – 485.

27. *Yoo, C.H., Kang, Y. J., Davidson, J. S.* Buckling analysis of curved beams by finite element discretization // J. Eng. Mech. ASCE. – 1996. – **122**, N 8. – P. 762 – 770.

APPENDIX

$$[C_o]^{-1} = \begin{bmatrix} 0 & -B_{o1}/R & B_{o2} & 0 & B_{o1}/R & B_{o3} \\ 0 & -B_{o5}/R & -B_{o4} & 0 & B_{o5}/R & -B_{o1} \\ 0 & B_{o4}/R & -B_{o2} & 0 & -B_{o1}/R & -B_{o3} \\ -1/b & 1/(R\,b) & 0 & 1/b & -1/(R\,b) & 0 \\ -1 & -B_{o1}/R & B_{o2} & 0 & B_{o1}/R & B_{o3} \\ 1/b & 2B_{o1}/(R\,b) & -B_{o1} & -1/b & -2B_{o1}/(R\,b) & -B_{o1} \end{bmatrix}; \qquad \text{(A.1)}$$

$$D_o = 2 - 2\cos f - b\sin f; \qquad \text{(A.2)}$$

$$B_{o1} = (\cos f - 1)/D_o; \qquad \text{(A.3)}$$

$$B_{o2} = \sin f / D_o; \qquad \text{(A.4)}$$

$$B_{o3} = (\sin f - f)/D_o \qquad \text{(A.5)}$$

$$B_{o4} = (1 - \cos f - f\sin f)/D_o; \qquad \text{(A.6)}$$

$$B_{o5} = \sin f / D_o; \qquad \text{(A.7)}$$

$$\{q_o\} = [C_o].\{a\}; \qquad \text{(A.8)}$$

$$\{a\} = \{a_1 \quad a_2 \quad a_3 \quad a_4 \quad a_5 \quad a_6\}; \qquad \text{(A.9)}$$

$$[P_1] = [R\cos f \quad R\sin f \quad R \quad -Rf \quad 0 \quad -Rf]; \qquad \text{(A.10)}$$

$$[P_2] = [\cos f \quad \sin f \quad 0 \quad 0 \quad -1 \quad -f]; \qquad \text{(A11)}$$

$$[P_3] = [-\sin f \quad \cos f \quad 0 \quad -1 \quad 0 \quad -1]; \qquad \text{(A12)}$$

$$[u] = [P_1][C_o]^{-1}\{q_o\}; \quad [q] = [P_2][C_o]^{-1}\{q_o\}; \quad [j] = [P_3][C_o]^{-1}\{q_o\}; \qquad \text{(A.13)}$$

$$[kk_o] = EI_z \int_0^{l_{sh}} \left(\left[P_1'' \right]^T \left[P_1'' \right] + 1/R \left[P_1'' \right]^T \left[P_2 \right] + 1/R \left[P_2 \right]^T \left[P_1'' \right] + 1/R \left[P_2 \right]^T \left[P_2 \right] \right) dy; \quad \text{(A.14)}$$

$$[mm_o] = \int_0^{l_{sh}} \left(r A \left[P_1 \right]^T \left[P_1 \right] + \left[P_2 \right]^T \left[P_2 \right] \right) dy; \quad \text{(A.15)}$$

$$\left[kk_{go} \right] = P(t) R \int_0^{l_{sh}} \left(\begin{array}{l} \left[P_1' \right]^T \left[P_1' \right] + r_x^2 \left[P_2' \right]^T \left[P_2' \right] + \\ r_z^2 \left(\left[P_2' \right]^T \left[P_2' \right] - 1/R \left[P_2' \right]^T \left[P_1' \right] - 1/R \left[P_1' \right]^T \left[P_2' \right] + 1/R \left[P_1' \right]^T \left[P_1' \right] \right) \end{array} \right) dy. \quad \text{(A.16)}$$

From the Editorial Board: The article corresponds completely to submitted manuscript.

Поступила 14.05.2009 Утверждена в печать 08.06.2010